12-20-1997

A Detailed Comparison of Hubble Space TelescopeFaint Object Spectrograph andIUEUltraviolet Spectra of Selected Seyfert Nuclei

Anuradha Koratkar
Space Telescope Science Institute

Ian Evans
Smithsonian Astrophysical Observator

Sharon Pesto
Space Telescope Science Institute

Cynthia Taylor
Dartmouth College

THE ASTROPHYSICAL JOURNAL, 491:536–544, 1997 December 20

A DETAILED COMPARISON OF *HUBBLE SPACE TELESCOPE* FAINT OBJECT SPECTROGRAPH AND *IUE* ULTRAVIOLET SPECTRA OF SELECTED SEYFERT NUCLEI

ANURADHA KORATKAR,[1] IAN EVANS,[2] SHARON PESTO,[1] AND CYNTHIA TAYLOR[3]
Received 1997 June 17; accepted 1997 August 4

ABSTRACT

Despite the contributions of the *Hubble Space Telescope* Faint Object Spectrograph (FOS) to the archive of UV observations of active galactic nuclei, the vast majority of UV reference data were obtained using the *International Ultraviolet Explorer* (*IUE*) satellite. These data remain important since they provide historical information about the intensities of the UV continua and emission lines that is needed to constrain models of the active nucleus. A detailed comparison of the FOS and *IUE* data is critical to understanding how the measurable quantities depend on the individual instrumental calibrations, and how any conclusions derived from modeling the observations may vary depending on the source of the UV data. Rigorous comparison of FOS and *IUE* spectra have so far been performed only for spectrophotometric standard star observations that are acquired accurately and have high signal-to-noise ratios. We compare typical FOS spectra that were not acquired and observed with the strict regimen that is used for standard-star observations, especially in the pre-COSTAR era.

All nonproprietary UV FOS spectrophotometric archival data for the Seyfert 1 galaxies Mrk 509, NGC 3783, and NGC 5548 that have near-simultaneous (within 24 hr) *IUE* observations are used in the analysis. These data demonstrate that the absolute photometric calibrations of the FOS and *IUE* agree within $\sim 5\%$ in absolute flux for two of the objects. For NGC 5548, the FOS and *IUE* flux data disagree by $\sim 50\%$ in the 1200–2000 Å region. In this object there may be evidence for flux nonlinearity of the *IUE* detector and a contribution from the host galaxy redward of 2800 Å. Cross-correlation of the FOS and *IUE* spectra reveals no zero-point wavelength shift larger than the *IUE* wavelength calibration errors. Comparison of line flux measurements from both the FOS and *IUE* spectra show that for strong emission lines (e.g., Lyα, C IV, and Mg II) the measured intensities always agree within 15%, while for moderately strong lines (e.g., N V, Si IV/O IV, He II, and C III]) the agreement is $\sim 30\%$ (1 σ). Weak lines (e.g., O I, C II, N IV], O III], and N III]) may not even be detected in the *IUE* spectra, and when they are detected the disagreement between the measured fluxes can be very large.

Subject headings: galaxies: active — galaxies: individual (Markarian 509, NGC 3783, NGC 5548) — galaxies: Seyfert — ultraviolet: galaxies

1. INTRODUCTION

Significant improvements to our understanding of the physical conditions found in active galaxies require the development of sophisticated numerical models that can predict in detail the emission from the nucleus. The reliability of such models depends critically on the accuracy with which measurements of the intensities of the UV continua and the many weak diagnostic UV lines, necessary to calibrate the models, can be performed. With the advent of the Faint Object Spectrograph (FOS) on board the *Hubble Space Telescope* (*HST*), weak UV emission lines visible in the spectra of active galactic nuclei (AGNs) can be measured with considerable accuracy.

Not only are accurate measurements of UV continua and emission lines important for constraining detailed models of the nucleus, but historical information about the line and continuum variability is equally significant. The *International Ultraviolet Explorer* (*IUE*) database of UV spectrophotometric observations is a major asset for these tasks. To effectively combine data from both the *HST* and *IUE* archives, a detailed comparison of the FOS and *IUE* absolute flux and wavelength calibrations is required.

Apart from calibration differences, the ability to measure accurately the line and continuum fluxes depends on the intrinsic nature of the data. The continuum level deduced from the spectra may be influenced significantly by the presence of weak lines in low signal-to-noise ratio (S/N) or low spectral resolution observations. Comparison of high-S/N, high-resolution FOS spectra with lower S/N, lower resolution *IUE* spectra allows an estimate of the magnitude of the error that can be introduced.

Rigorous comparison of the FOS and *IUE* UV photometric calibrations has so far been performed using three spectrophotometric standard stars (Colina & Bohlin 1994). These calibration observations have precision target acquisition sequences, and the spectra have very high S/N. Such data are not representative of typical FOS observations of an AGN, which often cannot be acquired with the same accuracy as standard stars, especially in the pre-COSTAR era. Furthermore, the UV flux from a typical AGN is several orders of magnitude fainter than from a spectrophotometric standard star. Flux-dependent effects in the *IUE* may need to be considered at these lower flux levels.

A search of the FOS and *IUE* archives reveals that there are three Seyfert galaxies (Mrk 509, NGC 3783, and NGC 5548) for which near-simultaneous (within 24 hr) observations are available. These spectra are well suited for com-

[1] Space Telescope Science Institute, 3700 San Martin Drive, Baltimore, MD 21218.
[2] Smithsonian Astrophysical Observatory, 60 Garden Street, MS-27, Cambridge, MA 02138.
[3] Department of Physics and Astronomy, Dartmouth College, 6127 Wilder Laboratory, Hanover, NH 03755.

paring the FOS and *IUE* flux calibrations for a typical AGN. In this paper we describe the most current recalibrations of the FOS and *IUE* spectra and discuss in detail the effects of the recalibration. We then perform an in-depth comparison of the spectra obtained by the two observatories.

2. DATA REDUCTION

2.1. *FOS Observations*

The FOS spectra of Mrk 509, NGC 3783, and NGC 5548 were retrieved from the *HST* data archive. All three targets were acquired by the FOS blue detector using a binary search target acquisition sequence into the 1″.0 circular aperture. Details of the observations are presented in Table 1.

The FOS spectra are recalibrated using the latest average inverse sensitivity (AIS) method calibration. This new method of flux-calibrating FOS data (1) normalizes count data from all apertures to the 4″.3 aperture to account for changes of aperture throughput as a function of the optical telescope assembly focus; (2) corrects the data for time-dependent detector sensitivity degradation; and (3) scales the data to the white dwarf reference scale. The AIS calibration method has been developed over a period of several years, with improvements applied progressively based on the observed performance of the calibration. Indeed, the final AIS calibration incorporates photometric corrections in the wavelength overlap regions of adjacent gratings reevaluated in light of inconsistencies discovered as a result of recalibrating over 1000 FOS spectra (Evans, Koratkar, & Pesto 1998). Details of the AIS technique can be found in Lindler & Bohlin (1994). Figure 1 demonstrates the difference between the archival and recalibrated spectra. For most pre-COSTAR data, recalibration yields an inferred flux that is of the order of 10%–40% higher than the original calibration. The most dramatic changes occur in the UV, because of the difference between the old and new photometric reference scales. We find that this is the case for the spectra analyzed here.

For each of the three objects, multiple observations obtained using the same grating are co-added to form a single spectrum for each wavelength region. The wavelength scales of the co-added spectra are shifted linearly so that the measured positions of Galactic absorption lines are at their vacuum rest wavelengths on average. The wavelength shifts applied to each of the co-added grating spectra are given in Table 1. For Mrk 509 and NGC 3783, there are several strong absorption lines per spectrum to determine accurately (0.2 Å) the wavelength shifts. For NGC 5548, fewer well-defined absorption lines are visible, but there is a sufficient number to determine the wavelength shifts to an accuracy of 0.4 Å. After the spectra are shifted in wavelength, they are combined to produce one master FOS spectrum per object.

Differences between the photometry in the wavelength overlap regions of adjacent gratings do not exceed 5% for the AIS-calibrated spectra. These differences are consistent with the overall photometric calibration of FOS spectra (Evans et al. 1998). Since the measured flux levels of the spectra in the grating overlap regions are consistent, the individual grating spectra are combined following the prescription of Evans et al. (1998). These combined, recalibrated FOS spectra are used in the following comparison with *IUE*.

2.2. *IUE Observations*

Low-resolution *IUE* spectra of Mrk 509, NGC 3783, and NGC 5548 were retrieved from the *IUE* archive. Details of the observations are given in Table 2.

The *IUE* spectra are recalibrated using the NEWSIPS technique (Nichols & Linsky 1996). The NEWSIPS calibration uses (1) a cross-correlation technique to register the science data, to reduce the pixel-to-pixel noise; (2) a single-

TABLE 1

FOS OBSERVATIONS

Object Name	Observation Date	Data Set Name	Grating	Exposure Time (s)	Wavelength Shift (Å)
Mrk 509	1992 Jun 21	Y0YA0302T	G130H	2100	0.0
		Y0YA0303T	G130H	2100	0.0
		Y0YA0304T	G190H	1620	0.3
		Y0YA0305T	G270H	600	0.4
NGC 3783.....	1992 Jul 27	Y10Z0103M	G190H	2100	0.9
		Y10Z0104M	G130H	1800	0.2
		Y10Z0105M	G130H	1800	0.2
NGC 5548.....	1992 Jul 5	Y0YA0202T	G130H	1650	0.7
		Y0YA0203T	G130H	1650	0.7
		Y0YA0204T	G190H	1200	1.7
		Y0YA0205T	G270H	480	1.8

TABLE 2

IUE OBSERVATIONS

Object Name	Observation Date	Data Set Name	Exposure Time (s)
Mrk 509	1992 Jun 22	SWP 44975	3000
		LWP 23353	2100
NGC 3783.....	1992 Jul 27	SWP 45237	5400
		LWP 23594	2700
NGC 5548.....	1992 Jul 5	SWP 45083	6600
		LWP 23450	3900

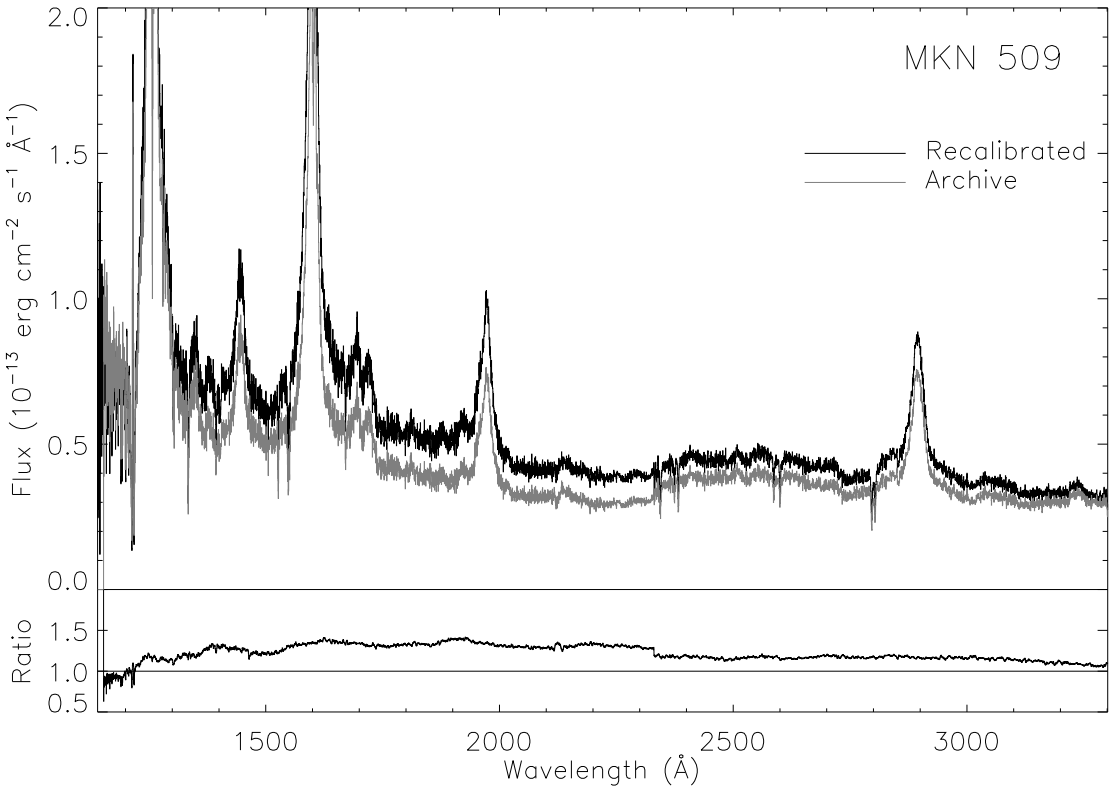

FIG. 1*a*

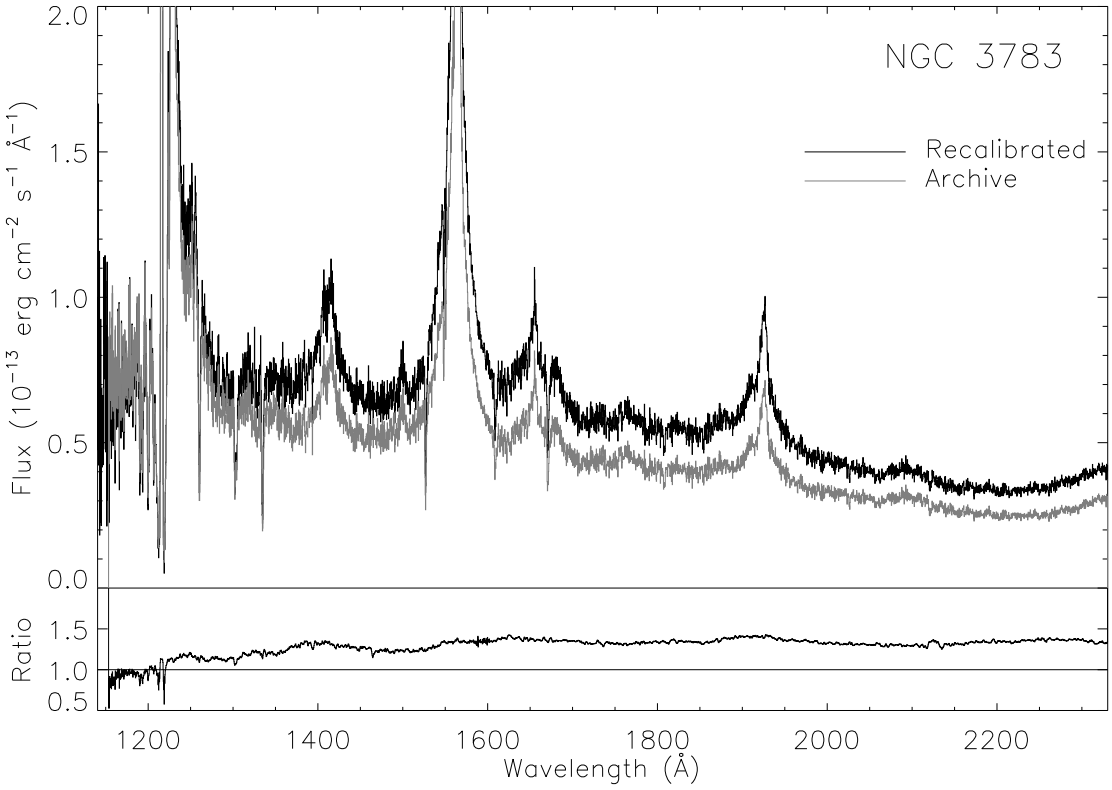

FIG. 1*b*

FIG. 1.—Difference between archival spectra (*gray line*) and spectra reprocessed (*dark line*) using the AIS calibration method. The lower plot in each panel shows the ratio of the recalibrated spectra to the spectra available in the archive. For most pre-COSTAR data, recalibration results in a change of the photometric calibration on the order of 10%–40%. The most dramatic changes occur in the UV because of the difference between the old (standard star) and new (white dwarf) photometric reference scales.

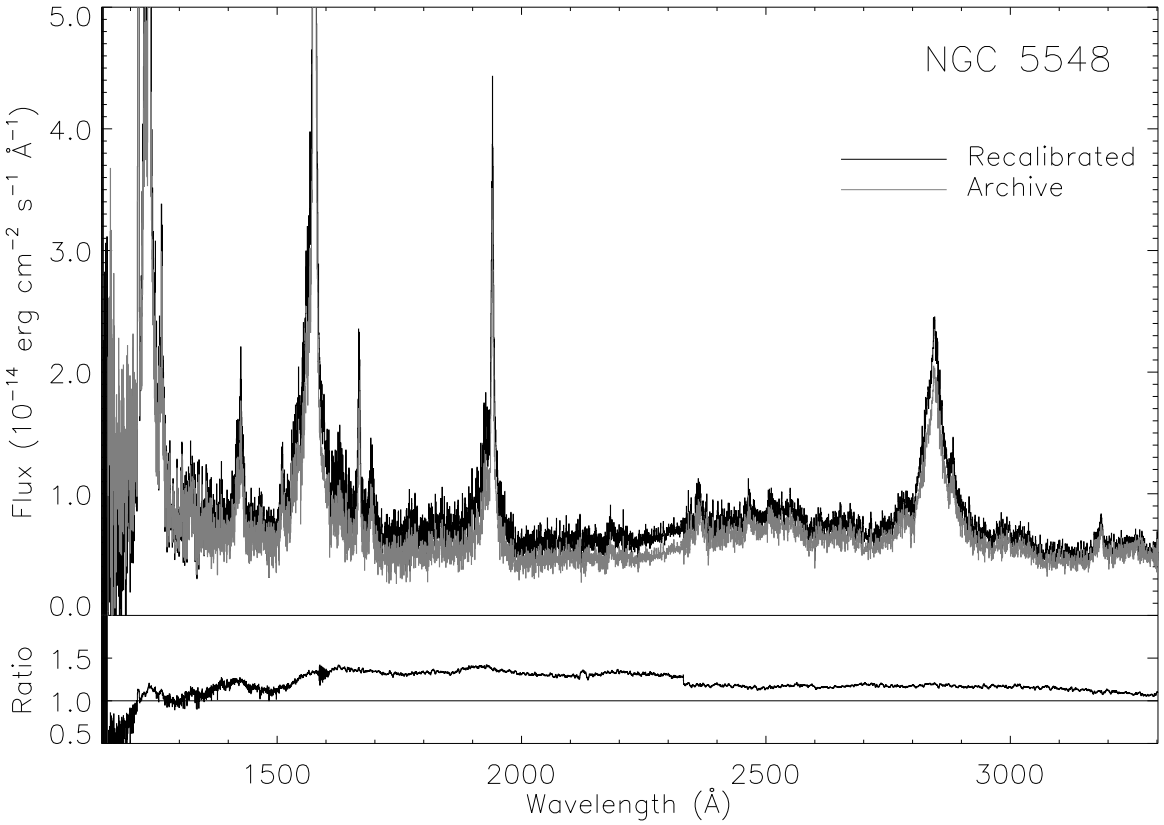

FIG. 1*c*

step geometric resampling (including all geometric corrections), to improve spectral resolution; (3) a slit-weighted extraction technique that incorporates a noise model, to improve S/N; and (4) new wavelength and absolute-flux calibrations that take into account the white dwarf photometric scale and temporal changes in sensitivity. The SWP and LWP spectra were *not* wavelength-shifted (unlike the *HST* data), because in most cases it is not possible to cleanly resolve the Galactic absorption lines given the S/N and lower resolution of the *IUE* spectra.

3. COMPARISON OF FOS AND *IUE* SPECTRA

3.1. *Wavelength Comparison*

Mapping of the *IUE* wavelength scale to the FOS wavelength scale is investigated by cross-correlating the FOS and *IUE* spectra. Table 3 shows the cross-correlation shifts required to align the strongest emission lines in the *IUE* spectra with the FOS data. The 1 σ FOS wavelength calibration errors are $\sim$0.1 Å for the G130H grating, $\sim$0.15 Å for the G190H grating, and $\sim$0.22 Å for the G270H grating. The apparent distortions in the *IUE* wavelength scale are most likely the result of errors introduced during the linearization of the dispersion relation. Although the formal 1 σ errors of the *IUE* wavelength calibration are $\sim$0.4 Å for the SWP camera and $\sim$0.6 Å for the LWP camera, the wavelength linearization procedure has associated wavelength-dependent non-Gaussian errors of the order of 0.5–1.5 pixels caused by second- and third-order terms. The wavelength calibration is determined from linearization of the *mean* fit to the dispersion relation, rather than from each individual spectrum. Consequently, some wavelength regions of individual spectra can have non-Gaussian wavelength calibration errors of order 2–3 Å (H. A. Bushouse 1997, private communication; M. Garhart 1997, private communication). Since the wavelength deviations that we observe are within the errors expected for the *IUE* wavelength calibration, no wavelength zero-point shift or nonlinear wavelength correction is applied to align the *IUE* and FOS spectra. The wavelength shifts applied to the FOS

TABLE 3

WAVELENGTH SHIFTS REQUIRED TO ALIGN *HST* AND *IUE* SPECTRA

Line	Shift[a] (Å)
Mrk 509:	
Lyα	2.1
Si IV/O IV	4.0
C IV	1.0
C III]	0.2
Mg II	2.1
NGC 3783:	
Lyα	−1.0
Si IV/O IV	−2.9
C IV	−0.7
C III]	−0.3
NGC 5548:	
Lyα	−0.8
Si IV/O IV	−4.9
C IV	−0.7
C III]	−1.9
Mg II	3.7

[a] The shift has to be added to the *IUE* data to align them with the FOS.

data to align the Galactic absorption lines with their rest wavelengths alter in detail the numerical results of the cross-correlation analysis, but they do not change this conclusion.

3.2. *Photometric Comparison*

Figure 2 compares the FOS and *IUE* spectra. In this figure, the recalibrated FOS spectra are resampled to the *IUE* wavelength grid and resolution using the STSDAS task RESAMPLE with sinc interpolation and a Hanning window. Figure 2 demonstrates that the absolute photometric calibrations of the FOS and *IUE* show some differences, even for this limited set of observations. Globally, for Mrk 509 and NGC 3783 the absolute photometry of the FOS and *IUE* agree within 5% $\pm$ 3%. A detailed inspection shows that the photometric agreement between FOS and *IUE* is independent of wavelength. Since the 1 σ absolute flux calibration errors in FOS and *IUE* are 3% and 5%, respectively, these observations are consistent with each other. For NGC 5548 the photometric differences are $\sim$50%.

Comparison of FOS and *IUE* spectra of three standard stars (Colina & Bohlin 1994) indicates that there is a difference of $\sim$6% between the absolute flux calibrations of the UV spectra and that the FOS calibration yields larger fluxes. For the spectra included in our comparison, the photometric calibrations do not produce larger flux values for the FOS observations. This may be the result of (1) inadequate aperture corrections, (2) target miscentering in the FOS aperture, or (3) nonlinearity of the *IUE* flux scale.

3.2.1. *Aperture Corrections*

In the present analysis we assume that the nuclear flux is emitted by a point source that is small compared with both the FOS and *IUE* apertures (and thus no correction for relative aperture area other than the aperture correction applied as part of the AIS-method calibration is needed). Although *HST* Wide Field Planetary Camera 2 (WFPC2) and Faint Object Camera (FOC) images of NGC 3783 and NGC 5548 confirm that both targets have compact, unresolved nuclei, the presence of faint extended UV continuum emission cannot be ruled out. Faint UV (2800 Å) continuum emission has been detected using the *HST* WFPC2 by Koratkar et al. (1998) in four low-luminosity AGNs. In those objects, only $\sim$10% of the *IUE* continuum flux comes from the nuclear point source, with the remainder produced by the surrounding galactic environment. Nevertheless, because of the extreme faintness of the extended continuum emission, it is only detectable in the *HST* WFPC2 images by integrating over the equivalent *IUE* aperture area. For the AGNs considered here, a contribution by even a very weak extended UV galaxy continuum too faint to be detected in the existing images could account for the few percent higher fluxes measured through the *IUE* aperture.

For NGC 5548 (which was observed during its faintest state), the *IUE* spectrum shows evidence for increasing flux redward of $\sim$2800 Å. Such a long-wavelength upturn may be the result of scattered sunlight. Another possibility is that the additional UV flux through the *IUE* aperture arises from a strong galactic bulge component. Existing UV FOC images of NGC 5548 are not sufficiently deep, and do not cover a large enough spatial extent, to detect directly any putative contribution from the extended galactic environment.

We therefore use the "AGN-free" aperture magnitudes for NGC 5548 from Romanishin et al. (1995; see also Peterson et al. 1995), combined with the observed UV-optical flux distribution of M32 as a galaxy bulge template to predict the approximate contribution from the galaxy bulge component in the 2800–3300 Å spectral region. Scaling the observed M32 flux in the B band to the Romanishin et al. (1995) "best AGN" AGN-free B magnitude in the *IUE* equivalent aperture, we estimate from the M32 template that the galaxy bulge contribution at 3250 Å is $\sim 5 \times 10^{-16}$ ergs^{-1} cm^{-2} Å^{-1}. This is an order of magnitude less than the difference between the FOS and *IUE* continuum fluxes at this wavelength. Substituting for the M32 template stellar models with spectral types F8–K0, corresponding approximately to the $B-V$ colors of the galaxy component in the inner several arcseconds of NGC 5548 (Romanishin et al. 1995, Table 1), yields mean predicted galaxy bulge fluxes of order (1–2.5) $\times 10^{-15}$ ergs^{-1} cm^{-2} Å^{-1} in the 3000–3300 Å waveband. The observed excess flux in the *IUE* aperture in this wavelength region is (4–8) $\times 10^{-15}$ ergs^{-1} cm^{-2} Å^{-1}. Consequently, it seems unlikely that the long wavelength upturn in the *IUE* data is caused solely by galaxy bulge.

It should be noted that neither scattered sunlight nor the galaxy bulge models above contribute sufficient flux shortward of 2000 Å to account for the discrepancy between the observed FOS and *IUE* UV fluxes at the shortest wavelengths.

3.2.2. *Target Miscentering*

Miscentering of a point-source target within an FOS aperture can alter the total flux deduced from pre-COSTAR observations, since some flux is lost irretrievably as a result of the nature of the pre-COSTAR *HST* point-spread function. The 1 σ pointing accuracy of the pre-COSTAR binary search target acquisition mode for the blue detector is $\sim$ 0.″12 (Vassiliadis et al. 1994). A careful analysis of the pre-COSTAR aperture throughputs for miscentered point-source targets shows that there is less than 2% loss in flux for target miscentering of this magnitude (Evans 1993; Bohlin 1993). Even severe target miscentering ($\sim$0.″3) in the FOS 1.″0 diameter circular aperture can account only for $\lesssim$10% loss of flux.

All three targets included in our analysis were acquired successfully by the FOS using the binary search target acquisition technique, and the target acquisition performance was verified using the binary search target acquisition simulator (Evans 1994). Consequently, we expect the pointing accuracy for our targets to be similar to the mean value found by Vassiliadis et al. (1994), implying that flux losses caused by target miscentering should be negligible. Since even severe miscentering of the target in the FOS aperture cannot account for the discrepancy between FOS and *IUE* fluxes for NGC 5548, we have not applied any photometric corrections to the data to adjust the fluxes.

3.2.3. *IUE Nonlinearity*

Nonlinearity in the *IUE* detectors is seen at low flux levels (M. Garhart 1997, private communication). Since the FOS Digicons count individual photons, nonlinearity is only a factor for very high count rates and does not occur at low flux levels. In NGC 5548, which has a continuum flux level of $\sim 6.5 \times 10^{-15}$ ergs^{-1} cm^{-2} Å^{-1}, the nonlinearity of the *IUE* could be significant. This nonlinearity is not suffi-

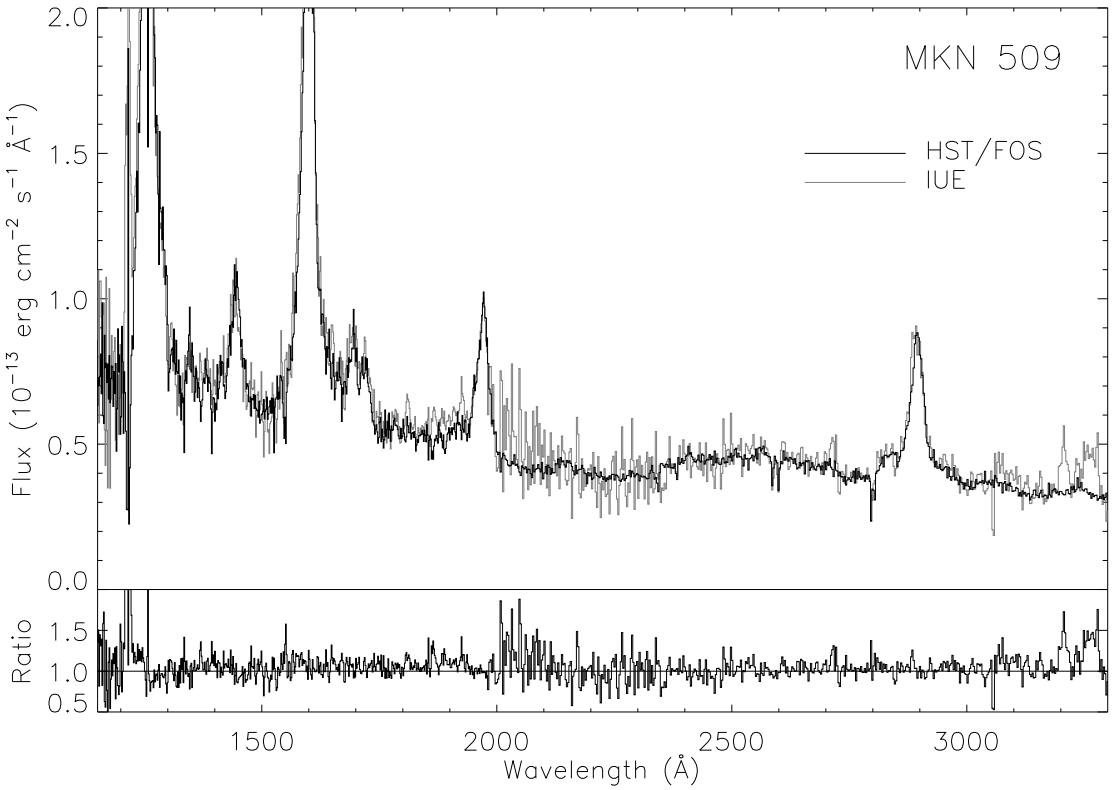

FIG. 2*a*

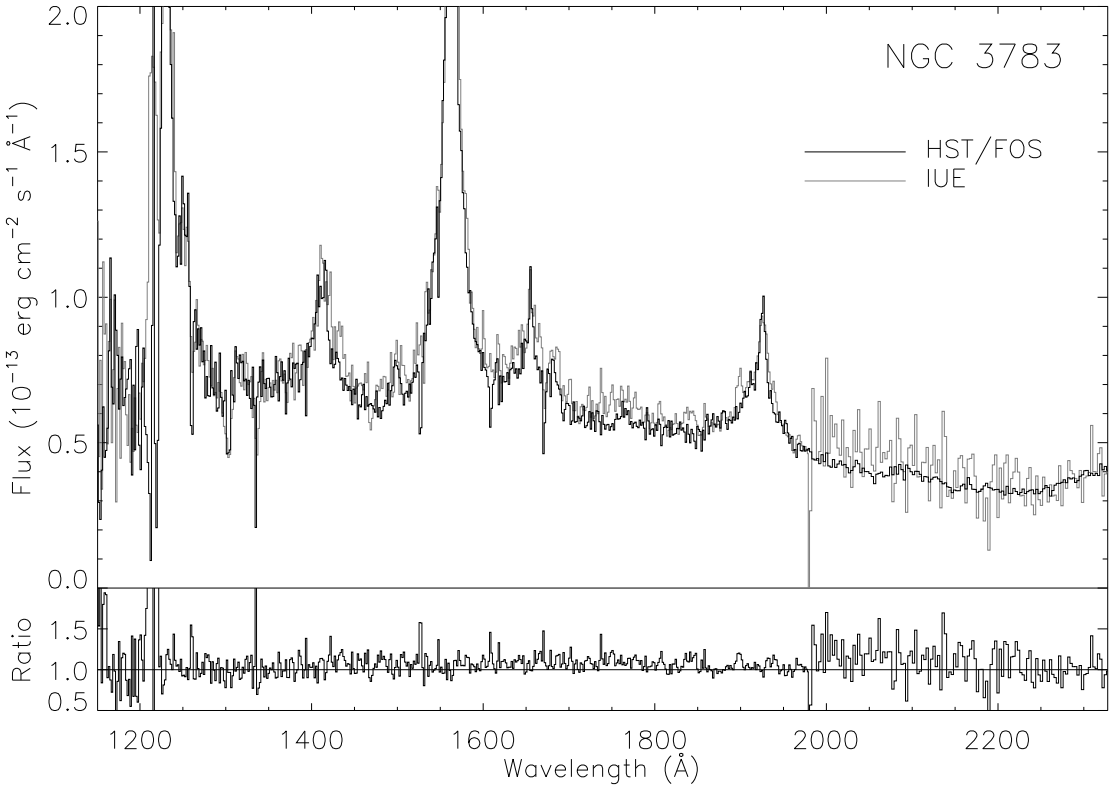

FIG. 2*b*

FIG. 2.—Comparison the FOS and *IUE* spectra. In this figure, the recalibrated FOS spectra are resampled to the *IUE* wavelength grid and resolution. The lower plot in each panel shows the ratio of the *IUE* spectrum to the FOS spectrum.

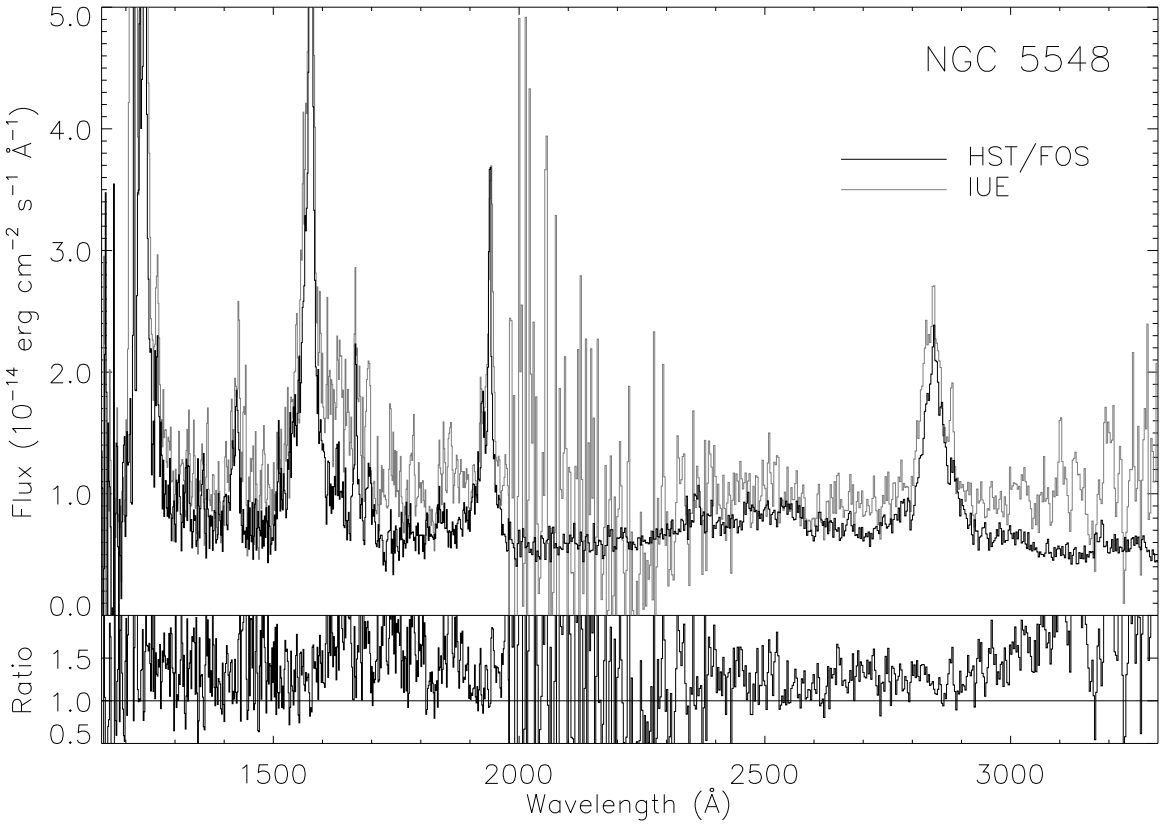

FIG. 2*c*

ciently well characterized to allow us to evaluate accurately its effect on the present data.

There is evidence in the *IUE* spectrum of NGC 5548 that the measured intensities of the wings of the strongest UV lines are higher relative to the peak line flux than is the case in the FOS data. We can speculate that this is the result of nonlinearity in the *IUE* detectors. If we hypothesize that this effect is solely responsible for the apparent enhancement of the measured continuum flux shortward of 2000 Å in the *IUE* spectrum, and further assume that the percentage flux overestimate is independent of wavelength to first order, then the majority of the "excess" flux in the *IUE* aperture longward of 2800 Å is accounted for by this effect. The remaining excess flux redward of 3000 Å in the *IUE* data is within a factor of 2 of the prediction for the galaxy bulge contribution with an F8 stellar model, and is most likely a combination of bulge and scattered sunlight components (see § 3.2.1).

Any one of the above effects by itself or in combination could easily account for the negligibly small difference between the FOS and *IUE* absolute photometry of Mrk 509 and NGC 3783.

3.3. *Line Measurements*

The accuracy with which line fluxes can be measured depends strongly on both the ability to properly position the underlying continuum and on the ability to distinguish cleanly the line from the continuum. This in turn depends on both the spectral resolution and the S/N of the data. For low-S/N data, weak emission lines or emission-line complexes such as Fe II may artificially raise the continuum. Line measurements that employ profile-fitting techniques can be adversely affected by low S/N and low spectral resolution, since the widths of the best-fitting profiles increase as the resolution degrades and the weak lines become less well distinguished from noisy continuum. Consequently, we should expect that for weak lines there may be significant differences between flux measurements from the FOS and *IUE* spectra. To quantify these effects, the intensities of a number of emission lines of different strengths are measured. In both the FOS and *IUE* spectra, the emission-line profiles are fitted using multiple Gaussian components, and the line fluxes are assumed to be equal to the sum of the fluxes of the contributing Gaussians. The line measurements are shown in Table 4, which also includes the ratio of measured *IUE* to FOS line fluxes.

For the three strongest emission lines (Lyα, C IV, and Mg II) in Mrk 509 and NGC 3783, the measured line fluxes always agree within 15%. However, for NGC 5548 the Lyα and C IV line fluxes appear to be overestimated by *IUE*. This overestimate may be the result of flux-dependent effects in the *IUE* calibration at the flux level of this extremely faint spectrum. Visual inspection of the strong line profiles in the *IUE* data indicates that the line wings appear to have significantly larger flux values in the *IUE* spectrum as compared with the FOS profiles, even though the peak flux is similar in both instruments. We additionally note that intrinsic absorption associated with the AGN can also lead to errors in the line intensity measurements when the spectral resolution is less than the absorption line width, and this source of error is seen in the case of Mrk 509.

For moderately strong lines (e.g., N V, Si IV/O IV, He II, and C III]), the *IUE* and FOS line fluxes agree within $\sim$30% (1 σ), with worst-case deviations of order 50% for the sample considered here. The measured *IUE* line fluxes can be either lower or higher than the line fluxes measured

TABLE 4

EMISSION-LINE INTENSITY MEASUREMENTS IN THE *HST* AND *IUE* SPECTRA

LINE	FLUX (10^{-13} ergs s^{-1} cm^{-2})		LINE RATIO (*IUE*/FOS)
	FOS	*IUE*	
Mrk 509:			
Lyα λ1215	86.77	95.95	1.11
N v λ1240	15.28	8.64	0.57
O i λ1302	3.13	1.89	0.61
C ii λ1334	1.23	5.51	4.46
Si iv/O iv λ1400	12.24	10.99	0.90
N iv] λ1486	0.67	0.00	0.00
C iv λ1550	76.03	84.05	1.11
He ii λ1640	9.29	10.48	1.13
O iii] λ1663	3.76	4.06	1.08
N iii] λ1753	0.51	1.05	2.07
Si ii λ1808	0.58	2.72	4.74
Al iii λ1854	3.00	3.18	1.06
C iii] λ1909	16.08	12.87	0.80
Mg ii λ2800	28.53	28.44	1.00
NGC 3783:			
Lyα λ1215	49.46	48.30	0.98
N v λ1240	6.31	4.08	0.65
O i λ1302	1.14	1.13	0.99
C ii λ1334	1.00	0.00	0.00
Si iv/O iv λ1400	10.79	14.67	1.36
N iv] λ1486	0.85	1.02	1.21
C iv λ1550	61.85	60.74	0.98
He ii λ1640	13.19	15.21	1.15
O iii] λ1663	0.85	1.12	1.32
N iii] λ1753	2.16	3.14	1.45
Si ii λ1808	1.65	0.00	0.00
Al iii λ1862	1.70	2.25	1.33
C iii] λ1909	14.91	13.16	0.88
NGC 5548:			
Lyα λ1215	17.59	22.31	1.27
N v λ1240	1.44	1.74	1.22
O i λ1302	0.61	1.75	2.86
C ii λ1334	0.22	0.00	0.00
Si iv/O iv λ1400	1.82	2.90	1.60
N iv] λ1486	0.22	0.00	0.00
C iv λ1550	18.67	23.77	1.27
He ii λ1640	1.86	1.76	0.95
O iii] λ1663	0.40	1.37	3.45
N iii] λ1753	0.31	0.87	2.85
Si ii λ1808	0.31	1.89	6.15
Si iii λ1892	0.18	0.72	4.09
C iii] λ1909	5.34	5.87	1.10
N ii λ2143	0.16	0.00	0.00
C ii λ2324	1.49	0.00	0.00
Mg ii λ2800	11.19	12.64	1.13

using the FOS, with about equal frequency. The fluxes measured for these lines are influenced both by S/N and by blending with nearby lines.

When detected in the *IUE* spectra, weak lines (e.g., O i, C ii, N iv], O iii], N iii]) can disagree by as much as a factor of 6. Nearly half of the weak lines detected in the *IUE* spectra have measured line fluxes ranging between 1.2 and 3.5 times the corresponding FOS fluxes. For these lines, both the S/N in the spectrum and spectral resolution dominate the line-fitting procedure. Typically, measurements of the *IUE* spectra imply more flux in the weak emission lines, because the width of the best-fitting Gaussian is much larger than for the FOS spectra, for which the lines are still well defined.

4. CONCLUSIONS

We have compared typical FOS and *IUE* UV spectra of three AGNs. These data demonstrate that the absolute photometric calibrations of the FOS and *IUE* are consistent, given the nature of the targets, exposures, and target acquisition. No wavelength shift is required to align the spectra, and the wavelength errors are consistent with the *IUE* wavelength calibration errors. Comparison of the emission line intensities for both the FOS and *IUE* spectra shows that the agreement between the line intensity measurements depends on the strength of the line. The strong emission lines agree within 15%. Moderately strong lines agree within $\sim$30% (1 σ). When detected in the *IUE* spectra, weak lines could have disagreements as large as a factor of 6.

The results in this paper are based on observations made with the NASA/ESA *Hubble Space Telescope*, obtained at the Space Telescope Science Institute, which is operated by the Association of Universities for Research in Astronomy, Inc., under NASA contract NAS 5-26555. A. K., I. E., and

S. P. would like to acknowledge support from NASA grant AR-4967. We thank C. Imhoff and M. Garhart for NEWSIPS-reprocessed *IUE* data and for answering numerous questions, and H. Bushouse for helpful discussions about the *IUE* wavelength calibration procedure. We also thank R. Bohlin and C. Keyes for energetic discussions of FOS calibration. The suggestions of an anonymous referee greatly improved the content of this paper.

REFERENCES

Bohlin, R. C. 1993, Light Loss in FOS as a Function of Pointing Error (Instr. Sci. Rep. CAL/FOS-097) (Baltimore: STScI)
Colina, L., & Bohlin, R. C. 1994, Comparison of the *HST*/FOS and IUE White Dwarf Absolute Flux Scales (Instr. Sci. Rep. CAL/SCS-003) (Baltimore: STScI)
Evans, I. N. 1993, Pre-COSTAR FOS Aperture Throughputs for Miscentered Targets Derived from PSF Models (Instr. Sci. Rep. CAL/FOS-107) (Baltimore: STScI)
———. 1994, The Faint Object Spectrograph Binary Search Target Acquisition Simulator BS4 (Instr. Sci. Rep. CAL/FOS-119) (Baltimore: STScI)
Evans, I. N., Koratkar, A., & Pesto, S. 1998, in preparation
Koratkar, A., et al. 1998, in preparation
Lindler, D. J., & Bohlin, R. C. 1994, Pre-COSTAR Photometric Calibration of the Faint Object Spectrograph (Instr. Sci. Rep. CAL/FOS-125) (Baltimore: STScI)
Nichols, J., & Linsky, J. L. 1996, AJ, 111, 517
Peterson, B. M., Pogge, R. W., Wanders, I., Smith, S. M., & Romanishin, W. 1995, PASP, 107, 579
Romanishin, W., et al. 1995, ApJ, 455, 516
Vassiliadis, E., Bohlin, R. C., Koratkar, A., & Evans, I. N. 1994, FOS Pre-COSTAR Blue Side: Target Acquisition Accuracy (Instr. Sci. Rep. CAL/FOS-122) (Baltimore: STScI)